CHAPTER 15

A Modified Method of Fundamental Solutions for Potential Flow Problems

Božidar Šarler[1]

Abstract. This chapter describes an application of the recently proposed Modified Method of Fundamental Solutions (MMFS) to the potential flow problems. The solution in two dimensional Cartesian coordinates is represented in terms of the fundamental solution of the Laplace equation together with the first order polynomial augmentation. The collocation is used for determination of the expansion coefficients. This novel method does not require fictitious boundary as the conventional Method of Fundamental Solutions (MFS). The source and collocation points thus coincide on the physical boundary of the system. The desingularised value of the fundamental solution in case of the coincidence of the collocation and source points is determined directly as the average value of the fundamental solution on the boundary in the vicinity of the source point. The respective values of the derivatives of the fundamental solution in the coordinate directions, as required in potential flow calculations, are calculated indirectly from the considerations of the constant potential field. The normal on the boundary is calculated by parametrisation of its length and use of the cubic radial basis functions with the second order polynomial augmentation. The components of the normal are calculated in an analytical way. A numerical example of potential flow around two dimensional circular region is shown. The results with the MMFS are compared with the results of the classical

[1] Laboratory for Multiphase Processes, University of Nova Gorica, Vipavska 13, SI-5000 Nova Gorica, Slovenia.

MFS and the analytical solution. It is shown that the MMFS gives better accuracy of the velocity components as compared with the classical MFS.

15.1 Introduction

The MFS is a numerical technique that falls in the class of methods generally called boundary methods. The other well known representative of these methods is the Boundary Element Method (BEM) [1]. Both methods are best applicable in situations where a fundamental solution to the partial differential equation in question is known. In such cases, the dimensionality of the discretization is reduced. BEM for example requires polygonisation of the boundary surfaces in general 3D cases, and boundary curves in general 2D cases. This method requires solution of the complicated regular, weakly singular, strongly singular, and hypersingular integrals over boundary segments which is usually a cumbersome and non-trivial task. The MFS has certain advantages over BEM, that are mostly visible in the fact that pointisation of the boundary is needed only, that completely avoids any integral evaluations, and makes no principal difference in coding between the 2D and the 3D cases. A comprehensive survey of the MFS and related methods for elliptic boundary value problems can be found in [2,3,4]. Some important developments of the MFS, that might be put into connection with the Laplace equation, focused in the present paper, are as follows. The method has been used for harmonic problems with linear [5] and non-linear boundary conditions [6], free boundaries [7,8], multi-domains [9], for heat conduction in isotropic and anisotropic bimaterials [10], and for axisymmetric problems [11]. The method has been expanded for material non-linearities and all technically relevant boundary conditions in a systematic way and applied to thermal design of hollow bricks [12]. The later paper represents one of the rare industrial applications of the MFS. In

the present paper, the potential flow problem, previously solved by the least squares version of MFS [13] and collocation version of MFS [8] is solved by the MMFS. This novel method, which essentially represents a sort of blend between BEM and MFS has been originally developed by [14] by using collocation with double layer Laplace equation fundamental solution. The method has been further extended to single-layer Laplace equation fundamental solution in [15]. The main drawback of the MFS represent positions of the source points that need to be positioned outside the boundary. In case they are too close to the boundary, the solution is not accurate. In case they are too far away from the boundary, the discretisation matrix becomes ill conditioned. The novel MMFS overcomes this difficulty by allowing the source point positions to coincide with the collocation points on the physical boundary. A desingularisation technique thus has to be employed in order to be able to allow bounded values in the discretisation matrix. The desingularisation has been derived through the properties of the double layer potential in [14] and through the indirect BEM formulation in [15]. In the present paper, the desingularisation is extended to the calculation of the desingularised values through the direct BEM approach, as well as to calculation of the desingularised value of the partial (not normal) derivatives on the boundary, which was not the case in previous two cited MMFS pioneering papers by the D.L. Young's group.

15.2. Governing Equations

Consider a connected two-dimensional domain Ω with boundary Γ. The domain is filled by a fluid that undergoes potential flow. The boundary is divided into the part Γ^E that represents external boundaries of the system and into the part Γ^I, that represents internal boundary of the system i.e. $\Gamma = \Gamma^E \cup \Gamma^I$. The potential Φ is governed by the following boundary value problem: Laplace equation

$$\nabla^2 \Phi = 0 , \tag{15.1}$$

and boundary conditions of the Dirichlet and Neumann type, located at the Dirichlet Γ^D and Neumann Γ^N parts of the boundary Γ, i.e. $\Gamma = \Gamma^D \cup \Gamma^N$

$$\Phi(\mathbf{p}) = \bar{\Phi}^D(\mathbf{p}), \quad \mathbf{p} \in \Gamma^D , \tag{15.2}$$

$$\frac{\partial \Phi}{\partial \mathbf{n}_\Gamma}(\mathbf{p}) = \bar{\Phi}^N(\mathbf{p}), \quad \mathbf{p} \in \Gamma^N , \tag{15.3}$$

with $\mathbf{p}$ standing for the position vector and $\mathbf{n}_\Gamma$ for the outward normal on the boundary Γ. $\bar{\Phi}^D$ and $\bar{\Phi}^N$ represent Dirichlet and Neumann boundary condition forcing functions. Let us introduce a two dimensional Cartesian coordinate system with ortho-normal base vectors $\mathbf{i}_x$ and $\mathbf{i}_y$ and coordinates p_x and p_y, i.e. $\mathbf{p} = p_x \mathbf{i}_x + p_y \mathbf{i}_y$. The potential field velocity components are calculated from the potential Φ as

$$v_\xi(\mathbf{p}) = \frac{\partial \Phi}{\partial p_\xi}(\mathbf{p}); \ \xi = x, y . \tag{15.4}$$

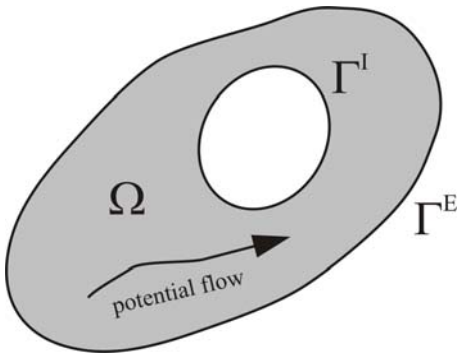

Fig. 15.1: Problem domain Ω with internal Γ^I and external Γ^E boundaries. Potential flow region is depicted in gray.

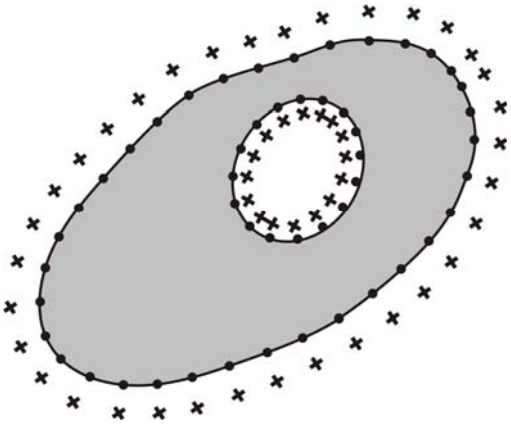

Fig. 15.2: Discretisation schematics. Symbols • and + represent collocation points and fundamental solution source points, respectively. These points do not coincide in the case of MFS(like in the figure) and coincide in the case of MMFS.

It is the purpose of this paper to determine the steady state potential flow components as a function of the posed geometry, governing equation and boundary conditions.

15.3. Solution Procedure

15.3.1 Solution of the Potential Flow

The common points of the MFS and MMFS for solution of the potential flow field are elaborated first. The differences are elaborated afterwards. The solution of the potential Φ is represented by the $N_\Gamma + 3$ global approximation functions $\psi_n^*(\mathbf{p})$ and their coefficients α_n^*

$$\Phi(\mathbf{p}) \approx \sum_{n=1}^{N_\Gamma+3} \psi_n^*(\mathbf{p})\alpha_n^*. \tag{15.5}$$

The global approximation functions have the property

$$\nabla^2 \psi_n^*(\mathbf{p}) = \begin{cases} 0; \mathbf{p} \neq \mathbf{p}_n \\ \delta(\mathbf{p}_n); \mathbf{p} = \mathbf{p}_n \end{cases}; n = 1, 2, ..., N_\Gamma, \tag{15.6}$$

i.e., they are fundamental solutions of the Laplace operator. δ denotes the Kronecker symbol. For two dimensional problems in Cartesian coordinates, the fundamental solution equals to

$$\begin{aligned} &\psi_n^*(\mathbf{p}) = \frac{1}{2\pi} \log \frac{r^*}{r_n}; \; r_n^2 = \mathbf{r}_n \cdot \mathbf{r}_n, \\ &\mathbf{r}_n = \mathbf{p} - \mathbf{s}_n = (p_x - s_{nx}) \mathbf{i}_x + (p_y - s_{ny}) \mathbf{i}_y \end{aligned} \tag{15.7}$$

for $n = 1, 2, ..., N_\Gamma$. The following three augmented functions (that also represent solution of the Laplace equation) can be additionally optionally introduced into the global approximation functions set

$$\psi_{N_\Gamma+1}^*(\mathbf{p}) = 1, \tag{15.8}$$

$$\psi_{N_\Gamma+2}^*(\mathbf{p}) = p_x - p_{0x}, \tag{15.9}$$

$$\psi_{N_\Gamma+3}^*(\mathbf{p}) = p_y - p_{0y}, \tag{15.10}$$

where r^* denotes the reference radius and p_{0x} and p_{0y} represent the mean coordinates of the $\Gamma \cup \Omega$. The augmentation functions have been introduced in order to be able to exactly satisfy possible constant or linear potential fields. Such global approximation functions set has been already successfully used in the calculation of the bubble shape in the potential flow (Šarler, 2006). Let us introduce the boundary condition indicators in order to be able to represent the boundary collocation equations in a compact form. The Dirichlet χ^D and Neumann χ^N type of boundary conditions indicators are

$$\chi^D(\mathbf{p}) = \begin{cases} 1; \mathbf{p} \in \Gamma^D \\ 0; \mathbf{p} \notin \Gamma^D \end{cases}, \tag{15.11}$$

$$\chi^N(\mathbf{p}) = \begin{cases} 1; \mathbf{p} \in \Gamma^N \\ 0; \mathbf{p} \notin \Gamma^N \end{cases}. \tag{15.12}$$

The coefficients are calculated from a system of $N_\Gamma + 3$ algebraic equations

$$\sum_{n=1}^{N_\Gamma+3} \Psi^*_{jn}\alpha^*_n = b_j;\ j = 1,2,...,N_\Gamma + 3\,. \tag{15.13}$$

The first N_Γ equations are obtained through collocation of Equation (5) in collocating points $\mathbf{p}_j; j = 1,2,...,N_\Gamma$ for $n = 1,2,...,N_\Gamma + 3$

$$\Psi^*_{jn} = \chi^D\left(\mathbf{p}_j\right)\psi^*_n\left(\mathbf{p}_j\right) + \chi^N\left(\mathbf{p}_j\right)\frac{\partial\psi^*_n}{\partial\mathbf{n}_\Gamma}\left(\mathbf{p}_j\right), \tag{15.14}$$

$$b_j = \chi^D\left(\mathbf{p}_j\right)\bar{\Phi}^D\left(\mathbf{p}_j\right) + \chi^N\left(\mathbf{p}_j\right)\frac{\partial\bar{\Phi}^N}{\partial\mathbf{n}_\Gamma}\left(\mathbf{p}_j\right), \tag{15.15}$$

and the remaining three equations $j = N_\Gamma + 1, N_\Gamma + 2, N_\Gamma + 3$ for $n = 1,2,...,N_\Gamma + 3$ are obtained through constraints

$$\Psi^*_{jn} = \Psi^*_{nj} = \psi^*_j\left(\mathbf{p}_n\right), \tag{15.16}$$

$$b_j = 0\,, \tag{15.17}$$

where the definition holds

$$\psi^*_n\left(\mathbf{p}_j\right) = 0;\quad j = N_\Gamma + 1, N_\Gamma + 2, N_\Gamma + 3\,. \tag{15.18}$$

The coefficients α^*_n can be expressed through inversion of the system (13), which gives

$$\alpha^*_n = \sum_{j=1}^{N_\Gamma} \Psi^{*-1}_{nj}\left[\chi^D\left(\mathbf{p}_j\right)\bar{\Phi}^D\left(\mathbf{p}_j\right) + \chi^N\left(\mathbf{p}_j\right)\bar{\Phi}^N\left(\mathbf{p}_j\right)\right];\quad n = 1,2,...,N_\Gamma + 3 \tag{15.19}$$

The velocity field components are calculated as

$$v_{\xi}(\mathbf{p}) = \sum_{j=1}^{N_\Gamma+3} \frac{\partial \psi_n^*}{\partial p_{\xi}}(\mathbf{p}) \alpha_n^*;\ \xi = x, y\,. \tag{15.20}$$

The explicit form of the partial derivatives of the fundamental solution are

$$\frac{\partial}{\partial p_{\xi}} f_n^*(\mathbf{p}) = -\frac{1}{2\pi} \frac{p_{\xi} - s_{n\xi}}{\left(p_x - s_{nx}\right)^2 + \left(p_y - s_{ny}\right)^2};\ \xi = x, y\ , \tag{15.21}$$

$$\frac{\partial}{\partial p_{\xi}} f_{N_\Gamma+1}^*(\mathbf{p}) = 0;\ \xi = x, y\ , \tag{15.22}$$

$$\frac{\partial}{\partial p_x} f_{N_\Gamma+2}^*(\mathbf{p}) = 1,\ \frac{\partial}{\partial p_y} f_{N_\Gamma+2}^*(\mathbf{p}) = 0\,, \tag{15.23}$$

$$\frac{\partial}{\partial p_x} f_{N_\Gamma+3}^*(\mathbf{p}) = 0,\ \frac{\partial}{\partial p_y} f_{N_\Gamma+3}^*(\mathbf{p}) = 1\,. \tag{15.24}$$

15.3.2 Classical Method of Fundamental Solutions

The fundamental solution source points are located outside physical boundary, i.e. $\mathbf{p}_j \neq \mathbf{s}_j$ and $\mathbf{s}_j \notin \Omega$ in the classical MFS. One can consider that they form an artificial boundary. The proper location of the source points is not a trivial task. It can be observed that the accuracy improves with the increasing distance from the physical boundary up to some extent. However, the collocation matrices become increasingly ill conditioned with increased distance from the boundary.

15.3.3 Modified Method of Fundamental Solutions

The key point of the modified method of fundamental solutions represents desingularisation of the value of the fundamental solution,

because in this case the source and the collocation points coincide, i.e. $\mathbf{p}_j = \mathbf{s}_j$. The desingularisation value can be directly set as an average value of the fundamental solution over a portion of the boundary. This can be formulated as

$$f_j^*\left(\mathbf{p}_j\right) = \frac{1}{\ell_j}\int_{\mathbf{p}_{j-1}}^{\mathbf{p}_j} f_j^*\left[\mathbf{p}(\Gamma)\right]d\Gamma + \frac{1}{\ell_{j+1}}\int_{\mathbf{p}_j}^{\mathbf{p}_{j+1}} f_j^*\left[\mathbf{p}(\Gamma)\right]d\Gamma\,. \tag{15.25}$$

The average value of the singularity at the boundary can be calculated in a closed form [16] from the direct BEM arsenal of analytical expressions

$$f_j^*\left(\mathbf{p}_j\right) = \frac{1}{4\pi}\left(1+\log\frac{2r^*}{\ell_j}\right) + \frac{1}{4\pi}\left(1+\log\frac{2r^*}{\ell_{j+1}}\right), \tag{15.26}$$

where ℓ_j represents the Euclidean distance between points $\mathbf{p}_{j-1}$ and $\mathbf{p}_j$ on the boundary. (For details see Section 3.4). The derivatives of the fundamental solution can be calculated in the following indirect way. Let us assume a pure Dirichlet problem with all the boundary values set to a constant $\overline{\Phi}^D\left(\mathbf{p}\right) = c;\ \mathbf{p}\in\Gamma$. We obtain in this case

$$\Phi\left(\mathbf{p}_j\right) = c = \sum_{n=1}^{N_\Gamma}\psi_n^*\left(\mathbf{p}_j\right)\alpha_n^c\,, \tag{15.27}$$

$$\frac{\partial}{\partial p_\xi}\Phi\left(\mathbf{p}_j\right) = \sum_{n=1}^{N_\Gamma+3}\frac{\partial}{\partial p_\xi}f_n^*\left(\mathbf{p}_j\right)\alpha_n^* = 0;\ \xi = x, y\,. \tag{15.28}$$

The desingularised value of the partial derivative can be calculated as

$$\frac{\partial}{\partial p_\xi} f_j^*\left(\mathbf{p}_j\right) = -\frac{1}{\alpha_j^c} \sum_{\substack{n=1 \\ n\neq j}}^{N_\Gamma} \frac{\partial}{\partial p_\xi} f_n^*\left(\mathbf{p}_j\right) \alpha_n^c; \xi = x, y\,. \tag{15.29}$$

The desingularised value of the normal derivative can be calculated from the desingularised values of the partial derivatives as

$$\frac{\partial}{\partial \mathbf{n}_\Gamma} f^*\left(\mathbf{p}_j\right) = \frac{\partial}{\partial p_x} f^*\left(\mathbf{p}_j\right) n_x\left(\mathbf{p}_j\right) + \frac{\partial}{\partial p_y} f^*\left(\mathbf{p}_j\right) n_y\left(\mathbf{p}_j\right). \tag{15.30}$$

15.3.4 Calculation of the Normal on the Boundary

The internal and external boundaries are given by a vector of points $\mathbf{p}_k; k = 1,2,...,N_\Gamma^B; B = I, E$. The length ℓ_k of the contour between the boundary points $\mathbf{p}_k$ and $\mathbf{p}_{k-1}$ is parametrised by the simple Euclidean distance

$$\ell_k = \left[\left(p_{kx} - p_{k-1x}\right)^2 + \left(p_{ky} - p_{k-1y}\right)^2\right]^{1/2}, \tag{15.31}$$

with the cyclic index conditions $k-1 = N_\Gamma^B;\ k = 1,\ k+1 = 1;\ k = N_\Gamma^B$. The total Euclidean length ℓ_Γ of the boundary contour equals to

$$\ell_\Gamma = \sum_{k=1}^{N_\Gamma^B} \ell_k\,. \tag{15.32}$$

The position of the boundary contour between the boundary points can be estimated by the meshless approximation with the contour parameter ℓ

$$p_\xi(\ell) = \sum_{k=1}^{N_\Gamma^B+3} \psi_k(\ell)\alpha_k^\xi;\ \xi = x, y\,. \tag{15.33}$$

The cubic splines

$$\psi_k(\ell) = \left|\ell - \ell_k\right|^3;\quad k = 1,2,...,N_\Gamma^B, \tag{15.34}$$

with the augmented functions

$$\psi_{N_\Gamma^B+1}(\ell)=1, \tag{15.35}$$

$$\psi_{N_\Gamma^B+2}(\ell)=\ell, \tag{15.36}$$

$$\psi_{N_\Gamma^B+3}(\ell)=\ell^2, \tag{15.37}$$

are used for the global approximation. The following three compatibility conditions are needed

$$\sum_{k=1}^{N_\Gamma^B+3}\psi_k(0)\alpha_k^\xi=\sum_{k=1}^{N_\Gamma^B+3}\psi_k(\ell_\Gamma)\alpha_k^\xi;\ \xi=x,y, \tag{15.38}$$

$$\sum_{k=1}^{N_\Gamma^B+3}\frac{d}{d\ell}\psi_k(0)\alpha_k^\xi=\sum_{k=1}^{N_\Gamma^B+3}\frac{d}{d\ell}\psi_k(\ell_\Gamma)\alpha_k^\xi;\ \xi=x,y, \tag{15.39}$$

$$\sum_{k=1}^{N_\Gamma^B+3}\frac{d^2}{d\ell^2}\psi_k(0)\alpha_k^\xi=\sum_{k=1}^{N_\Gamma^B+3}\frac{d^2}{d\ell^2}\psi_k(\ell_\Gamma)\alpha_k^\xi;\ \xi=x,y, \tag{15.40}$$

in order to ensure the continuity and the smoothness of the first and the second derivatives required in calculation of the bubble normal and curvature. The coefficients are calculated from a system of N_Γ^B+3 algebraic equations

$$\sum_{n=1}^{N_\Gamma^B+3}\Psi_{kn}\alpha_n^\xi=b_k^\xi;\quad n=1,2,...,N_\Gamma^B+3,\ \xi=x,y. \tag{15.41}$$

The first N_Γ^B equations are obtained through collocation of Eq. (34) for x and y directions in collocation points $\ell_k;k=1,2,...,N_\Gamma^B$ for $n=1,2,...,N_\Gamma^B+3$, distributed over Γ^B

$$\Psi_{kn}^\xi=\psi_n(\ell_k);\ \xi=x,y, \tag{15.42}$$

$$b_k^\xi=p_{k\xi};\ \xi=x,y. \tag{15.43}$$

The remaining 3 equations are obtained through the compatibility conditions

$$\Psi^{\xi}_{\left(N_{\Gamma}^{B}+1\right)n} = \psi_n\left(\ell_{\Gamma}\right) - \psi_n\left(0\right);\ \xi = x, y\,, \tag{15.44}$$

$$b_k^{\xi} = 0;\ k = N_{\Gamma}^{B} + 1,\ \xi = x, y\,, \tag{15.45}$$

$$\Psi^{\xi}_{\left(N_{\Gamma}^{B}+2\right)n} = \frac{d\psi_k}{d\ell}\left(\ell_{\Gamma}\right) - \frac{d\psi_k}{d\ell}\left(0\right);\quad \xi = x, y\,, \tag{15.46}$$

$$b_k^{\xi} = 0;\ k = N_{\Gamma}^{B} + 2,\ \xi = x, y\,, \tag{15.47}$$

$$\Psi^{\xi}_{\left(N_{\Gamma}^{B}+3\right)n} = \frac{d^2\psi_n}{d\ell^2}\left(\ell_{\Gamma}\right) - \frac{d^2\psi_n}{d\ell^2}\left(0\right);\quad \xi = x, y\,, \tag{15.48}$$

$$b_k^{\xi} = 0;\ k = N_{\Gamma}^{B} + 3\,. \tag{15.49}$$

The coefficients α_n^x and α_n^y can be expressed through inversion of the related two systems (15.41)

$$\alpha_n^{\xi} = \sum_{k=1}^{N_{\Gamma}^{B}} \Psi_{nk}^{\xi-1} p_k^{\xi};\ \xi = x, y\,. \tag{15.50}$$

The components of the normal on the boundary can be explicitly calculated as

$$n_{\Gamma x} = +\frac{dp_y}{d\ell}\left[\left(\frac{dp_x}{d\ell}\right)^2 + \left(\frac{dp_y}{d\ell}\right)^2\right]^{-1/2}, \tag{15.51}$$

$$n_{\Gamma y} = -\frac{dp_x}{d\ell}\left[\left(\frac{dp_x}{d\ell}\right)^2 + \left(\frac{dp_y}{d\ell}\right)^2\right]^{-1/2}. \tag{15.52}$$

15.4. Numerical Examples

Potential flow arround a circle is considered for a numerical example. The flow is confined to a square (exterior) region Γ^E, $p_x^- \le p_x \le p_x^+$, $p_y^- \le p_y \le p_y^+$ with $p_x^+ = -p_x^- = p_0$, $p_y^+ = -p_y^- = p_0$. The Dirichlet boundary conditions are defined at the square boundaries as

$$\bar{\Phi}^D\left(p_x, p_y\right) = v_0 p_y;\ p_x = p_x^{\pm},\ p_y = p_y^{\pm}. \tag{15.53}$$

The potential field, defined from the boundary conditions (44) gives the following solution for the velocity field

$$v_{0x} = 0, \tag{15.54}$$

$$v_{0y} = v_0. \tag{15.55}$$

A circular hole Γ^I (internal boundary) with the radius r_0, centered around point $\mathbf{p}_c$ with coordinates $p_{cx} = \left(p_x^+ + p_x^-\right)/2$, $p_{cy} = \left(p_y^+ + p_y^-\right)/2$ with the Neumann boundary conditions

$$\bar{\Phi}^N\left[p_x\left(\Gamma^I\right), p_y\left(\Gamma^I\right)\right] = 0;\ \mathbf{p} \in \Gamma^I \tag{15.56}$$

is inserted into the square. The solution of the potential field is for $r_0 \ll p_0$ equal to

$$\Phi_{\text{ana}} = v_{0y}\left(p_y - p_{cy}\right)\left[1 + \frac{r_0^2}{\left(p_x - p_{cx}\right)^2 + \left(p_y - p_{cy}\right)^2}\right], \tag{15.57}$$

with v_{0y} defined from equation (15.55). The respective analytical solution for the velocity field is

$$v_{\text{ana}\,x} = -v_{0x}\frac{2v_{0y}r_0^2\left(p_x - p_{cx}\right)\left(p_y - p_{cy}\right)}{\left(p_x - p_{cx}\right)^2 + \left(p_y - p_{cy}\right)^2}, \tag{15.58}$$

$$v_{\text{ana}\,y} = v_{0x}\left[1 + \frac{r_0^2}{\left(p_x - p_{cx}\right)^2 + \left(p_y - p_{cy}\right)^2}\right] - \frac{2v_{0y}r_0^2\left(p_y - p_{cy}\right)^2}{\left(p_x - p_{cx}\right)^2 + \left(p_y - p_{cy}\right)^2}. \tag{15.59}$$

We set $r_0 = 0.1\,\text{m}$ and $p_0 = 0.5\,\text{m}$ for defining the geometry. The square

sides are virtually divided into 50 equal length segments and the collocation points are put at each of the segment centers. The total number of discretisation points on the external boundary is set to $N^E = 200$. The circle is discretised by five different discretisations $N^I = 8,16,32,64,128$. In case of the MFS, the source points are moved for 5 nodal distances in the direction of the outward normal on the external boundary. In case of the internal boundary, the source point boundaries are put on the artificial boundary with radius $r_{0s} < r_0$. The distances between the source points on this boundary and the distances between the source points and corresponding collocation points are assumed to be the same, i.e.

$$r_0 - r_{0s} = 2\pi r_{0s} / N^I . \tag{15.60}$$

From this equation, the radius of the circle on which the source points are set, is calculated as

$$r_{0s} = \frac{r_0}{1 + \dfrac{2\pi}{N^I}} . \tag{15.61}$$

In the MMFS, the source points are coincident with the boundary points. The Root Mean Square (RMS) error of the MFS and MMFS solutions are defined as

$$\Phi_{\text{rms}} = \sum_{n=1}^{N^I} \left\{ \frac{1}{N^I} \left[\Phi(\mathbf{p}_n) - \Phi_{\text{ana}}(\mathbf{p}_n) \right]^2 \right\}^{1/2} , \tag{15.62}$$

$$v_{\xi\,\text{rms}} = \sum_{n=1}^{N^I} \left\{ \frac{1}{N^I} \left[v_\xi(\mathbf{p}_n) - v_{\xi\,\text{ana}}(\mathbf{p}_n) \right]^2 \right\}^{1/2} ; \xi = x, y , \tag{15.63}$$

$$v_{\text{rms}} = \left(v_{x\,\text{rms}}^2 + v_{y\,\text{rms}}^2 \right)^{1/2} . \tag{15.64}$$

The RMS errors of the potential, velocity components, and absolute value of velocity are in case of MFS given in Table 1 as a function of the discretisation density N^I. One can observe monotone convergence of the

results with finer discretisation. Similar results are given in Table 2 for MMFS. The calculated potential is in the case of MFS calculated more accurately as in the case of MMFS for $N^I = 8,16$. The velocity components and absolute value of velocity are better predicted by MMFS than in MFS in all attempted discretisations.

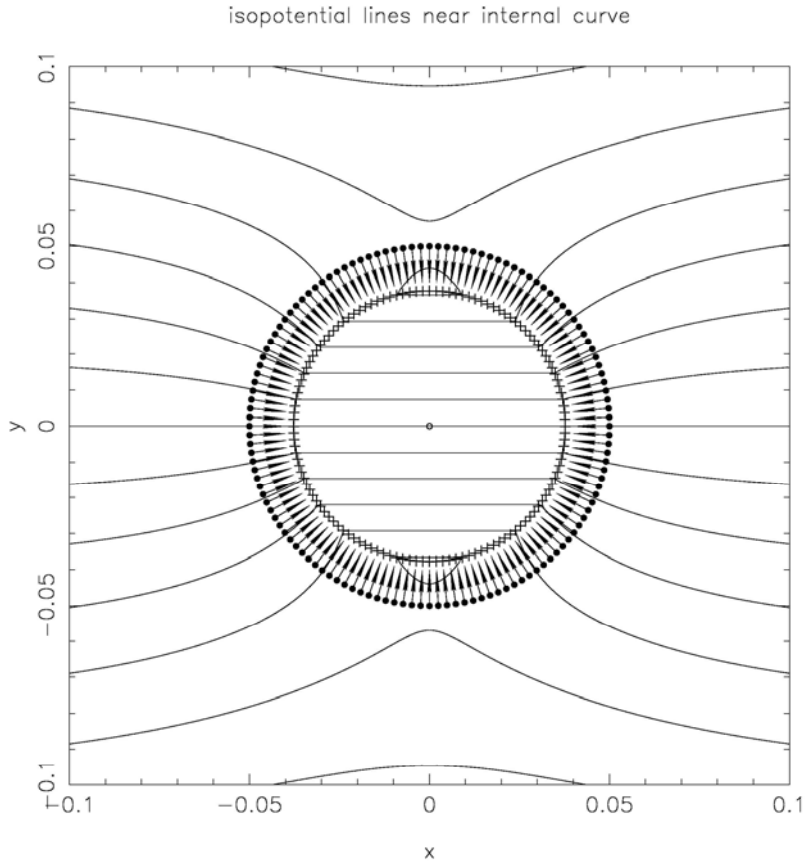

Fig. 3a: Potential around circle. MFS. Note the artificial boundary. The normals are calculated through Eqs. (15.51,15.52).

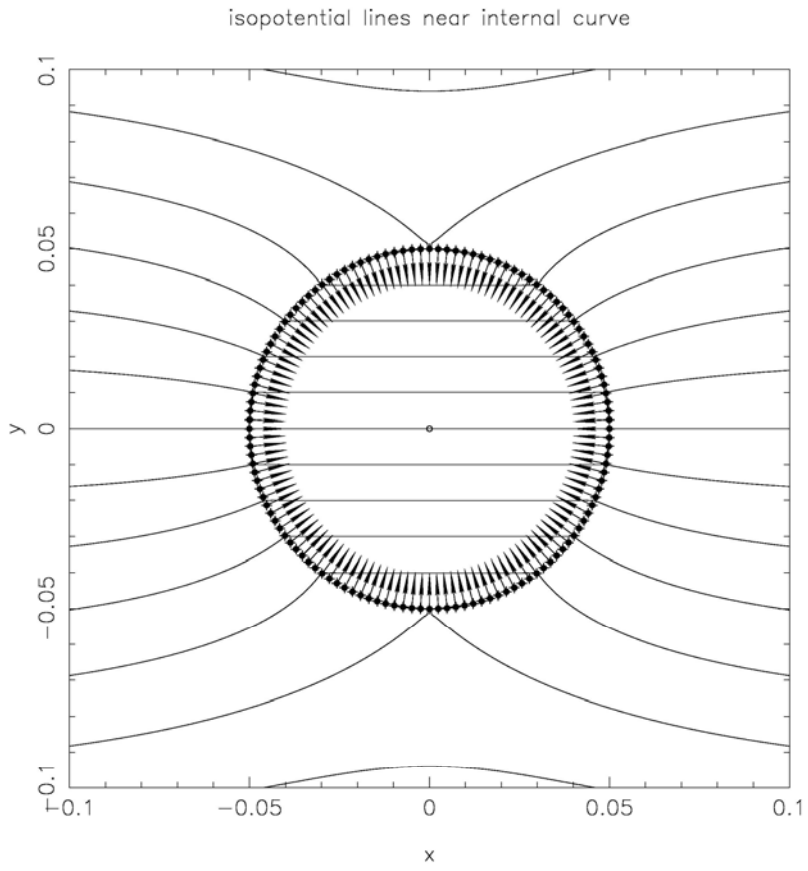

Fig. 3b: Potential around circle. MMFS. Note the absence of artificial boundary. The normals are calculated through Eqs. (15.51,15.52).

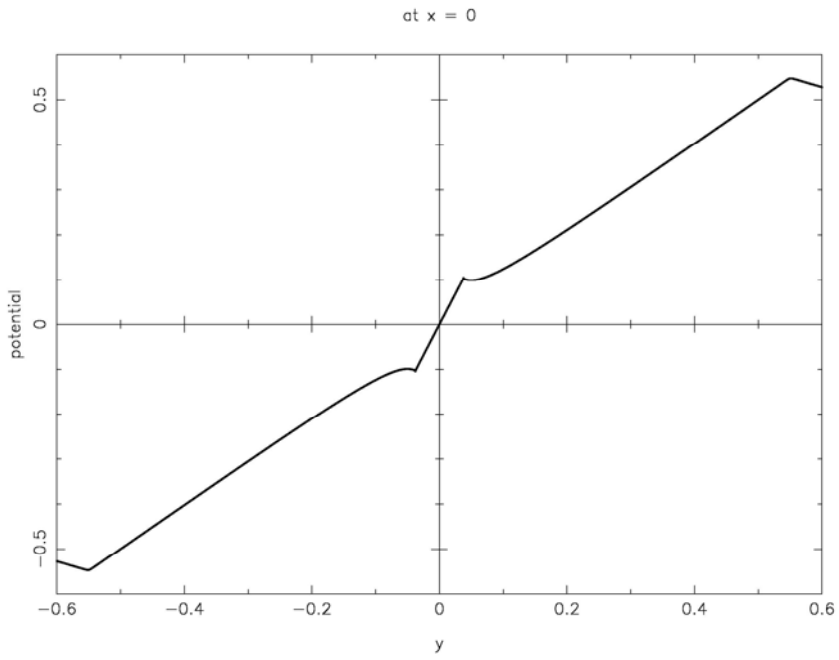

Fig. 4a: Calculated potential as a function of the square height at the square centerline. MFS. The jump in the derivative coincides with the artificial boundary position.

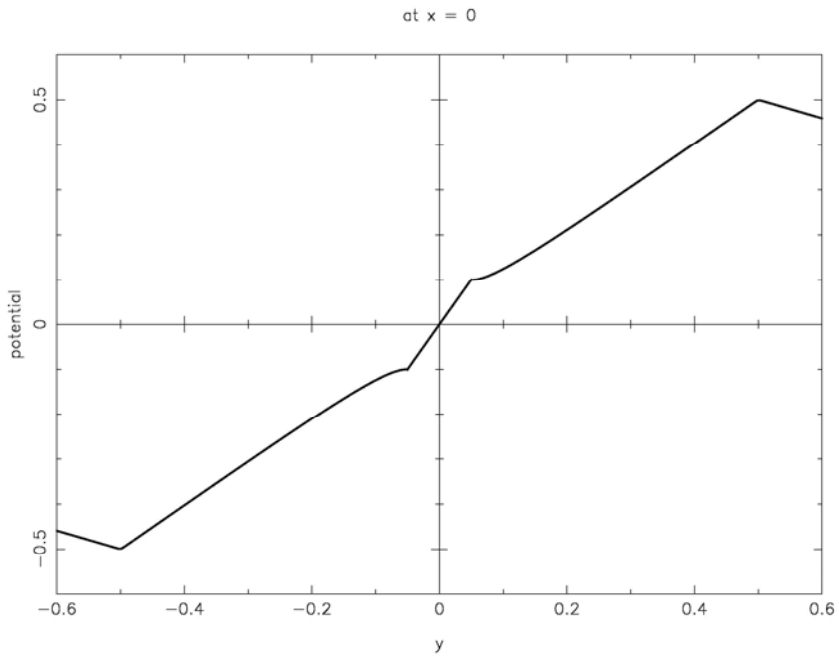

Fig. 4b: Calculated potential as a function of the square height at the square centerline. MMFS. The jump in the derivative coincides with the physical boundary position.

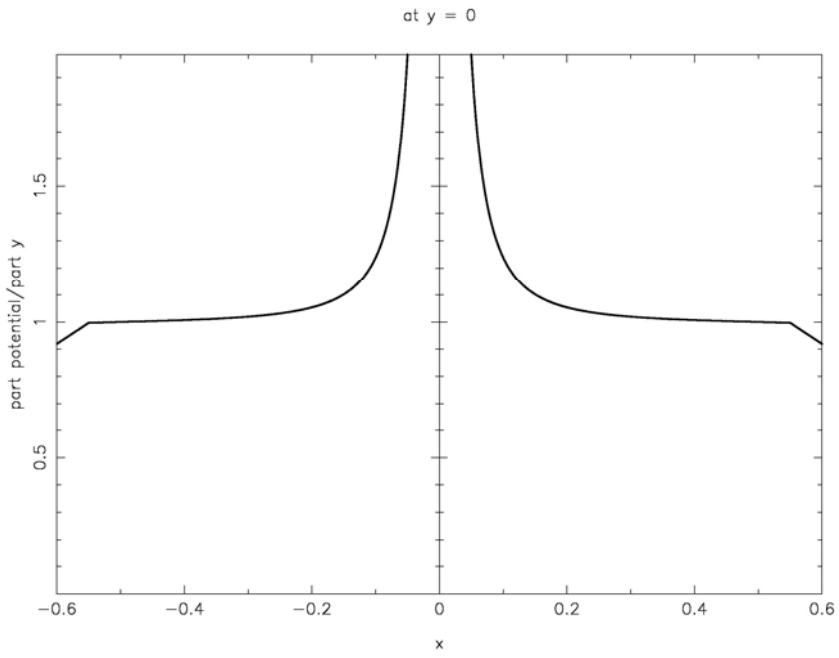

Fig. 5a: Calculated potential as a function of the square width at the square centerline. MFS.

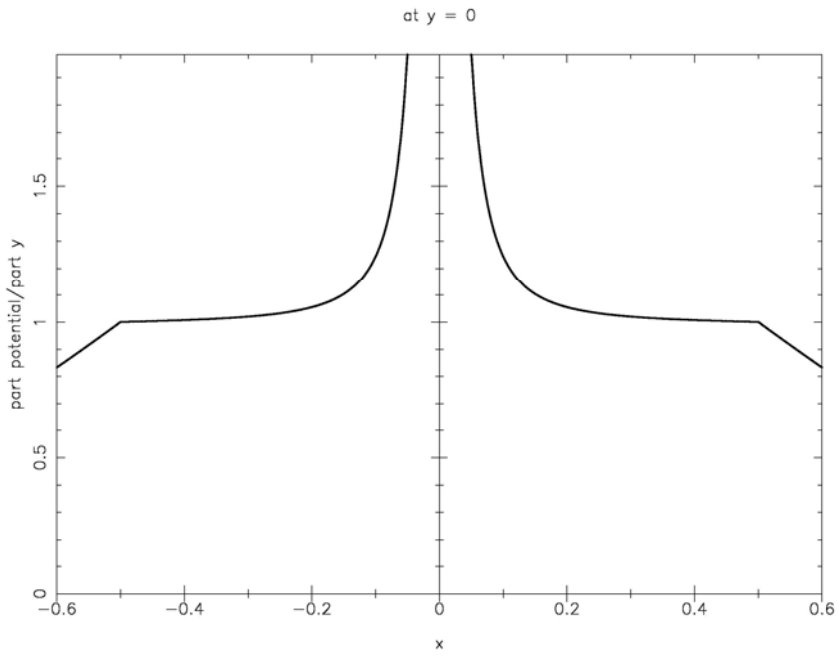

Fig. 5b: Calculated potential as a function of the square width at the square centerline. MMFS.

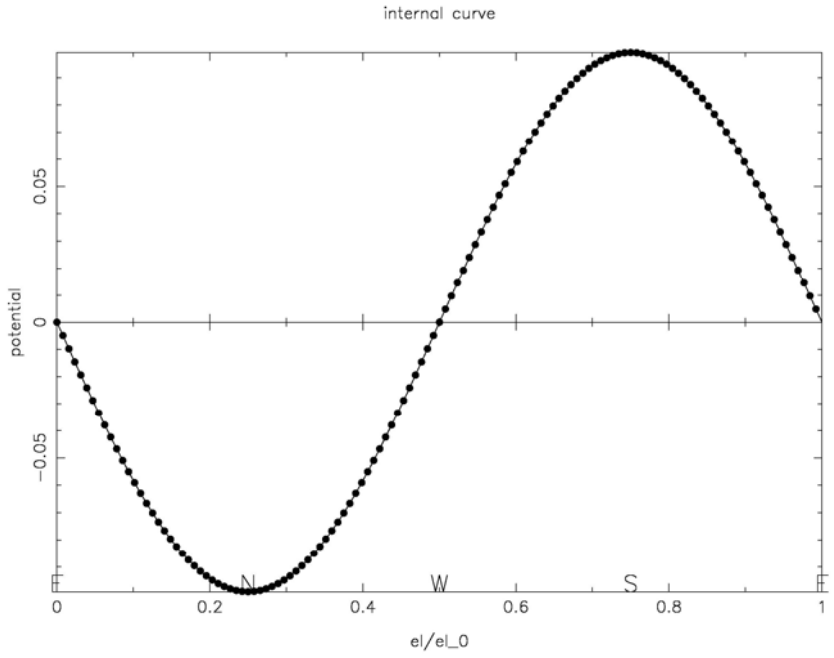

Fig. 6: Calculated potential on the circle. MMFS.

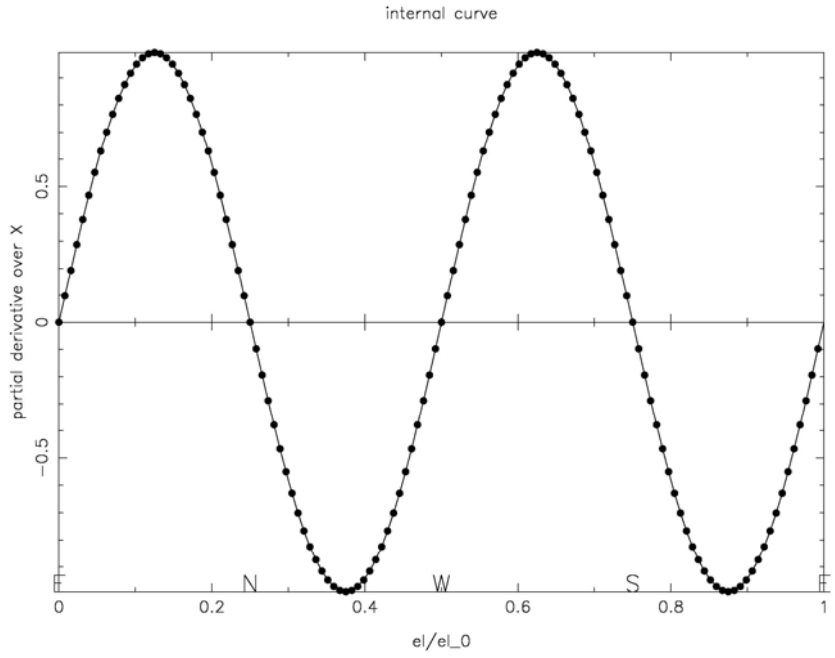

Fig. 7: Calculated x component of the velocity on the circle. MMFS.

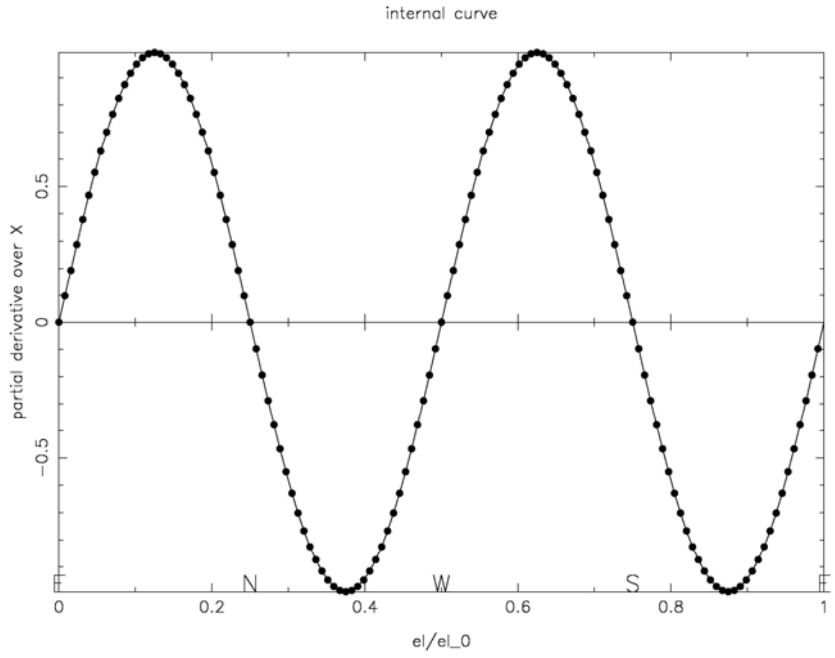

Fig. 8: Calculated y component of the velocity on the circle. MMFS.

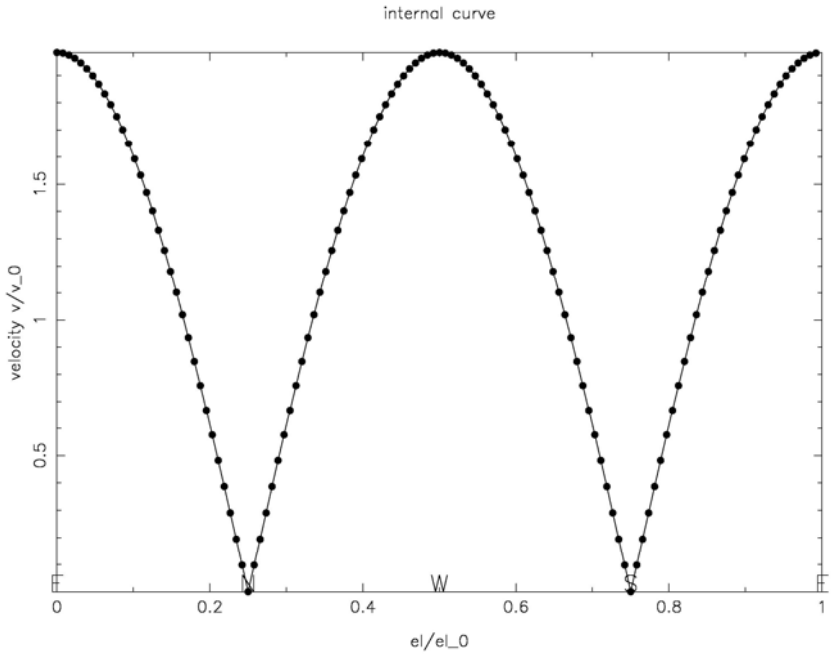

Fig. 9: Calculated absolute value of the velocity on the circle. MMFS.

Tab.15.1: RMS error of the MFS as a function of the circle discretisation.

N^I	Φ_{rms}	$v_{x\text{rms}}$	$v_{y\text{rms}}$	v_{rms}
8	2.5518376E-03	3.9154895E-02	6.7793891E-02	7.8288674E-02
16	2.9815510E-03	3.7008923E-02	6.4071439E-02	7.3991954E-02
32	3.2131092E-03	3.5812065E-02	6.1997332E-02	7.1597300E-02
64	3.3342016E-03	3.5207942E-02	6.0950622E-02	7.0388757E-02
128	3.3961909E-03	3.4906309E-02	6.0428046E-02	6.9785379E-02

Tab. 15.2: RMS error of the MMFS as a function of the circle discretisation.

N^I	Φ_{rms}	$v_{x\text{rms}}$	$v_{y\text{rms}}$	v_{rms}
8	9.7905844E-03	7.1186870E-03	1.2311025E-02	1.4221007E-02
16	3.7417179E-03	5.9746308E-03	1.0346274E-02	1.1947452E-02
32	1.4548693E-03	5.5269711E-03	9.5522050E-03	1.1035942E-02
64	4.3769614E-04	5.3238771E-03	9.1936914E-03	1.0623918E-02
128	4.4850865E-05	5.2269851E-03	9.0229781E-03	1.0427632E-02

15.5. Conclusions

The MFS represents a numerical technique best applicable in situations where the fundamental solution of the partial differential equation is known. In recent years, the MFS has proved to be an effective alternative to the boundary element methods in specific problems. Due to its advantages with respect to the simplicity of formulation and the fact that the distribution of the calculation nodes is truly meshless, the method is an ideal candidate for

the moving and free boundary problems. Its main drawback represents the "artificial boundary issue". This issue has been in this work overcome through the MMFS concept. The desingularisation has been in the present work made in a direct BEM sense. The desingularisation of the spatial derivatives has been made in an indirect way through the constant potential field concept. Both approaches differ from the previous two pioneering works on the subject [14,15]. In addition, this paper extends the MMFS to potential flow situations. The components of the flow field are calculated more precisely with the MMFS as with the MFS at all discretisations used. The presented developments can be straightforwardly upgraded to axisymmetric problems [11] by inclusion of the axisymmetric fundamental solution. The flow physics can be extended to Navier-Stokes flow by the strategy, proposed in [17] which uses the dual reciprocity with radial basis functions. The axisymmetric radial basis functions, such as thin plate splines [18] and multiquadrics [19] can be used for this purpose in axisymmetry.

Acknowledgement

This paper forms a part of the project J2-0099: Multiscale Modelling and Simulation of Liquid-Solid Systems, sponsored by the Slovenian Research Agency. The financial support is kindly acknowledged.

References

[1] L.C. Wrobel, M.H. Aliabadi, *The Boundary Element Method*, J.Wiley, Chichester, 2002.

[2] G. Fairweather, A. Karageorghis, The method of fundamental solutions for elliptic boundary value problems, *Advances in Computational Mathematics,* 9:69-95, 1998.

[3] M.A. Golberg, C.S. Chen, Discrete Projection Methods for Integral Equations, CMP, Southampton, 1997.

[4] M.A. Golberg, C.S. Chen, The method of fundamental solutions for potential, Helmholtz and diffusion problems, *Boundary Integral Methods - Numerical and Mathematical Aspects*, ed. M.A Golberg, CMP, Southampton, 103-176, 1998.

[5] R.T. Fenner, Source field superposition analysis of two dimensional potential problems, *International Journal of Numerical Methods in Engineering*, 32:1079–1091, 1991.

[6] A. Karagheorgis, G. Fairweather, The Method of Fundamental Solutions for the solution of nonlinear plane potential problems, *IMA Journal of Numerical Analysis*, 9:231–242, 1989.

[7] A. Karageorghis, The Method of Fundamental Solutions for the solution of steady state free boundary problems, *Journal of Computational Physics*, 98:119–128, 1992.

[8] B. Šarler, Solution of a two-dimensional bubble shape in potential flow by the method of fundamental solutions, *Engineering Analysis with Boundary Elements*, 30:227-235, 2006.

[9] V.M.A. Leitao, On the implementation of a multi-region Trefftz-collocation formulation for 2-D potential problems, *Engineering Analysis with Boundary Elements*, 20:51–61, 1997.

[10] J.R. Berger, A. Karageorghis, The Method of Fundamental Solutions for heat conduction in layered materials, *International Journal for Numerical Methods in Engineering*, 45:1618–1694, 1999.

[11] A. Karageorghis, G. Fairweather, The method of fundamental solutions for axisymmetric potential problems, *International Journal of Numerical Methods in Engineering*, 44:1653–1669, 1999.

[12] B. Šarler, R. Vertnik, M. Savić, C.S. Chen, A meshless approach to hollow-brick temperature field, *Advances in Computational Engineering & Sciences*, ed. Atluri, S.N.; Pepper, D.W., Tech Science Press, Encinio, 6 pages, 2002.

[13] R.L. Johnston, G. Fairweather, The method of fundamental solutions for problems in potential flow, *Applied Mathematical Modelling*, 8:265-270, 1984.

[14] D.L. Young, K.H. Chen, C.W. Lee, Novel meshless method for solving the potential problems with arbitrary domain, *Journal of Computational Physics*, 209:290-322, 2005.

[15] D.L. Young, J.T. Chen, J.H. Kao, A modified method of fundamental solutions with source on the boundary for solving Laplace equations with circular and arbitrary domains, *CMES: Computer Modelling in Engineering and Sciences*, 19:197-221, 2007.

[16] Z. Rek, B. Šarler, Analytical integration of elliptic 2D fundamental solution and its derivatives for straight-line elements with constant interpolation, *Engineering Analysis with Boundary Elements*, 5-6:515-525, 1999.

[17] B. Šarler, Towards a mesh-free solution of transport phenomena, *Engineering Analysis with Boundary Elements,* 26:731-738, 2002.

[18] B. Šarler, Axisymmetric augmented thin plate splines, *Engineering Analysis with Boundary Elements,* 21:81-85, 1998.

[19] B. Šarler, N. Jelić, I. Kovačević, M. Lakner, J. Perko, Axisymmetric multiquadrics, *Engineering Analysis with Boundary Elements,* 30:137-142, 2006.